Electronic Supplementary Material (ESI) for Journal of Materials Chemistry A.

Supporting information

Layered Nickel metal-organic framework for high performance alkaline battery-supercapacitor hybrid deceives

Yang Jiao, Jian Pei*, Chunshuang Yan, Dahong Chen, Yongyuan Hu, Gang Chen*

MIIT Key Laboratory of Critical Materials Technology for New Energy Conversion and Storage, School of Chemistry and Chemical Engineering, Harbin Institute of Technology, Harbin 150001, People's Republic of China

To whom correspondences should be addressed: E-mail: peijian008@163.com and gchen@hit.edu.cn

Table S1 Comparison of specific capacity among the previous reports and our works using the three-electrode system.

Electrode materials	Electrolyte	Current density ($A \cdot g^{-1}$)	Specific capacity ($mAh \cdot g^{-1}$)	Ref.
CoS nanowire arrays	2 M KOH	2	129	S1
Co_3O_4 nanosheets	6 M KOH	1	20.2	S2
MoS_2 nanosheets/ Graphene	1 M Na_2SO_4	0.1	75	S3
NiO Nanofibers	6 M KOH	2	25.3	S4
Porous Graphene Framework	3 M KOH	0.2	66	S5
Ni-MOF	3 M KOH	1	123	Our Work
Ni-MOF	3 M KOH + 0.1 M $K_4Fe(CN)_6$	1	175	Our Work

Table S2 Various performance parameters for our ABSHD in 3 M KOH electrolyte.

Current density ($A \cdot g^{-1}$)	Discharge time (s)	Specific capacity ($mAh \cdot g^{-1}$)	Energy density ($W \cdot h \cdot kg^{-1}$)	Power density ($W \cdot kg^{-1}$)
1	277.2	77	53.9	700
2	113.6	63.1	44.2	1400
5	42.5	59	41.4	3500
10	20.4	56.7	39.7	7000

Table S3 Various performance parameters for our ABSHD in 3 M KOH and 0.1M $K_4Fe(CN)_6$ electrolyte.

Current density ($A \cdot g^{-1}$)	Discharge time(s)	Specific capacity ($mAh \cdot g^{-1}$)	Energy density ($W \cdot h \cdot kg^{-1}$)	Power density ($W \cdot kg^{-1}$)
1	348	96.7	67.7	700
2	163.3	90.7	63.5	1400
5	62	85.5	60.3	3500
10	28.7	79.8	55.8	7000

Table S4 Comparison of electrochemistry performance of electrochemical energy stored devices fabricated in our work with others reported.

Materials	Counter	Electrolyte	Potential Window (V)	Energy Density ($W \cdot h \cdot Kg^{-1}$)	Power Density ($W \cdot Kg^{-1}$)	Ref.
MnO_2	AC	0.5 M Na_2SO_4	1.8	10.4	14700	S6
Co_3O_4@$Ni(OH)_2$	RGO	6 M KOH	1.6	18.54	1860	S7
$Ni(OH)_2$@ Ni foam	a-MEGO	6 M KOH	1.8	13.4	85000	S8
$Co(OH)_2$ nanorods	GO	1 M KOH	1.2	11.94	2540	S9
MnO_2	AC	0.5 M K_2SO_4	1.8	28.4	150	S10
Ni-MOF	CNTs-COOH	3 M KOH	1.4	39.7	7000	Our Work
Ni-MOF	CNTs-COOH	3 M KOH + 0.1 M $K_4Fe(CN)_6$	1.4	55.8	7000	Our Work

AC: activated carbon
RGO: graphene
a-MEGO: activated microwave exfoliated graphite oxide
GO: graphene oxide
CNTs-COOH: carbon nanotubes functionlized with carboxylic group

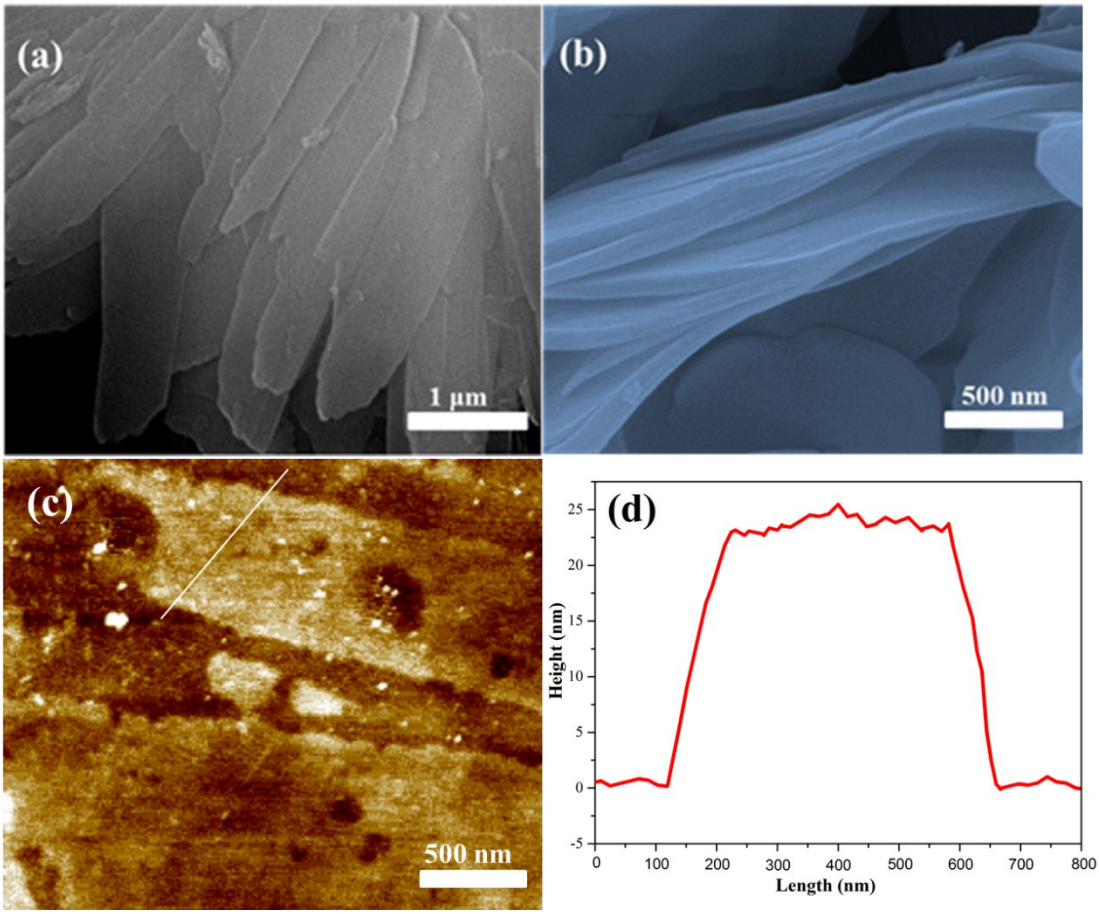

Figure S1 (a, b) SEM images of Ni-MOF. (c) AFM image of the layered Ni-MOF nanosheets and (d) corresponding height profile.

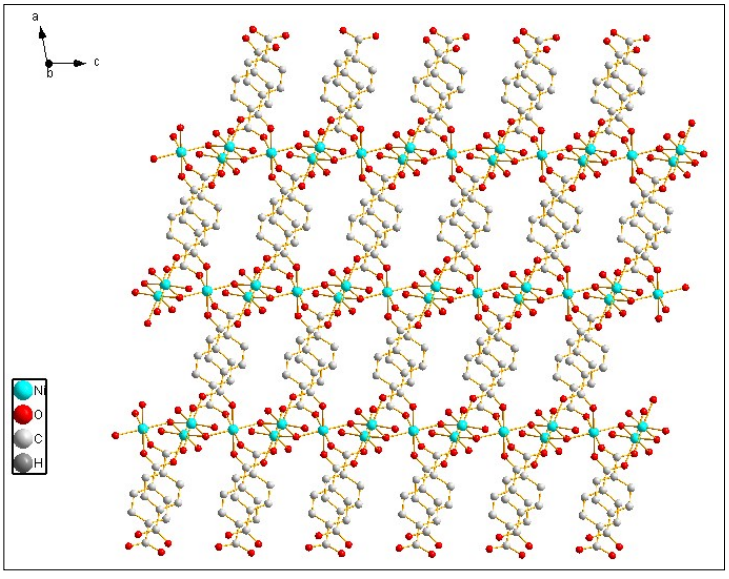

Figure S2 View of the structure of Ni-MOF along the b axis.

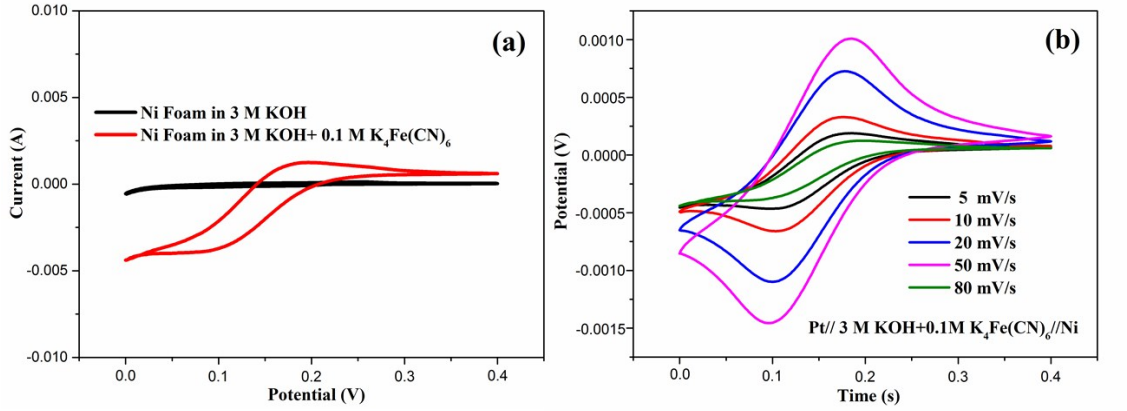

Figure S3 (a) Cyclic voltammograms of Ni foam and Ni-MOF in 3 M KOH + 0.1 M $K_4Fe(CN)_6$ at a scan rate of 5 mV s^{-1}. (b) CV curves of bare Ni foam as working electrode at different scan rates.

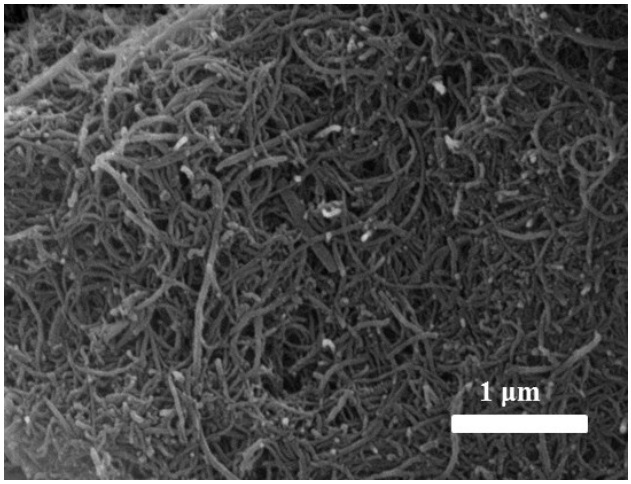

Figure S4 SEM image of the CNTs-COOH.

Preparation of negative electrode and its electrochemical performances:

The negative electrode for the alkaline battery-supercapacitor hybrid device (ABSHD) was prepared by mixing Carbon nanotubes functionlized with carboxylic group (CNTs-COOH), carbon black, polyvinylene difluoride (PVDF) (in the weight ratio of 8:1:1) together using NMP as solvent. The mixture was coated onto the cleaned Ni foam (1 cm^2) and was kept for drying at 80 °C overnight. Then the electrode was used as the working electrode. 3 M KOH solution, saturated calomel electrode (SCE) and platinum foil were used as the electrolytes, reference and counter electrodes, respectively. The weight of active material is about 4 mg. The specific capacitance of CNTs-COOH is 156.7 F g^{-1} at the current density of 1 A g^{-1}. Moreover, grapheme oxide (GO) was also used as another negative electrode for the ABSHD. The specific capacitance of GO is 91.6 F g^{-1} at the current density of 1 A g^{-1}. The Ni-MOF//GO ABSHD in 3 M KOH exhibit energy density of 33 W h kg^{-1} at a power density of 7000 W kg^{-1}. This result indicated that the high electrochemical performance is independent with the negative electrode, and support the high electrochemical performance of Ni-MOF.

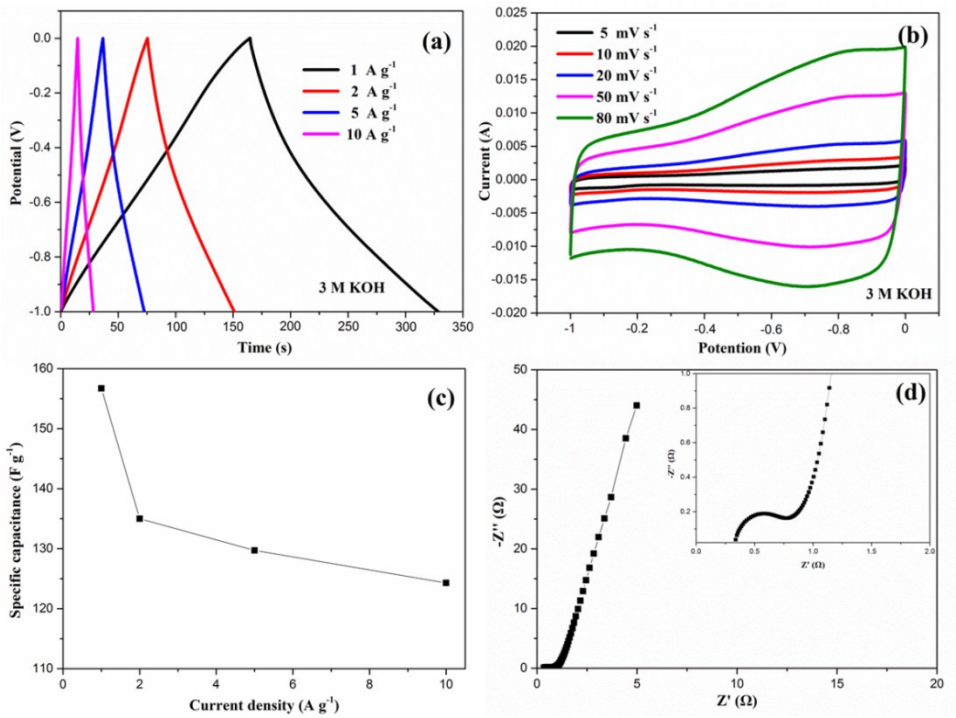

Figure S5 (a) Charge and discharge curves of CNTs-COOH at different current densities ranged from 1 to 10 A g^{-1}. (b) CV curves of CNTs-COOH at the scan rate between 5 and 80 mV s^{-1}. (c) Specific capacity as a function of current density. (d) Nyquist plots of the CNTs-COOH

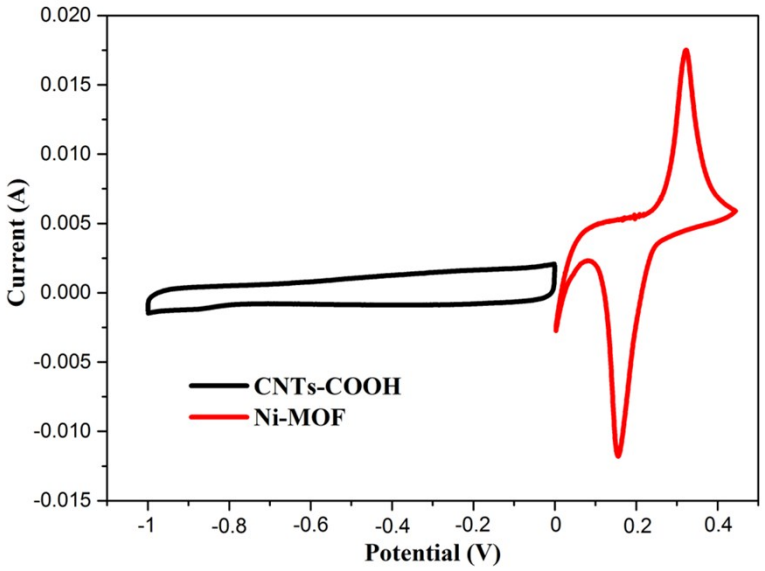

Figure S6 CV curves of Ni-MOF and CNTs-COOH electrodes performed in a three-electrode cell in a 3 M KOH + 0.1 M $K_4Fe(CN)_6$ electrolyte at a scan rate of 5 mV s^{-1}.

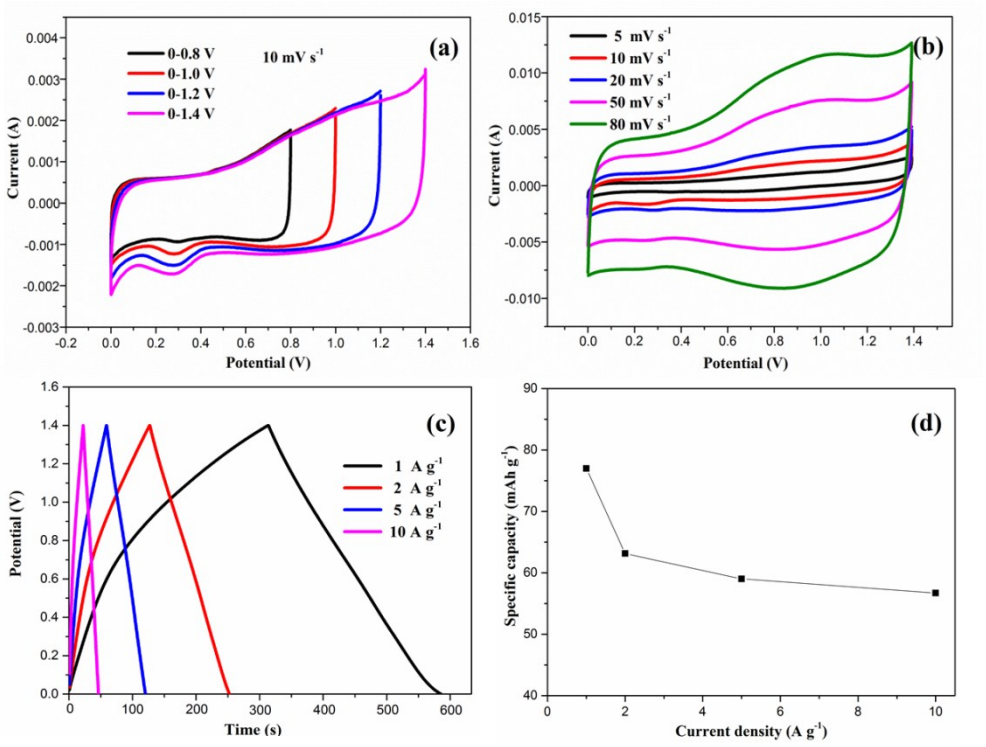

Figure S7 (a) CV curves of the optimized Ni-MOF//CNTs-COOH ABSHD in 3 M KOH was collected at different potential windows at a scan rate of 10 mV s^{-1}. (b) CV curves of the optimized Ni-MOF//CNTs-COOH ABSHD in 3 M KOH collected at various scan rates. (c) Charge–discharge curves of optimized Ni-MOF//CNTs-COOH ABSHD in 3 M KOH collected at various current densities. (d) Plot of the current density against the specific capacity of Ni-MOF//CNTs-COOH ABSHD in 3 M KOH.

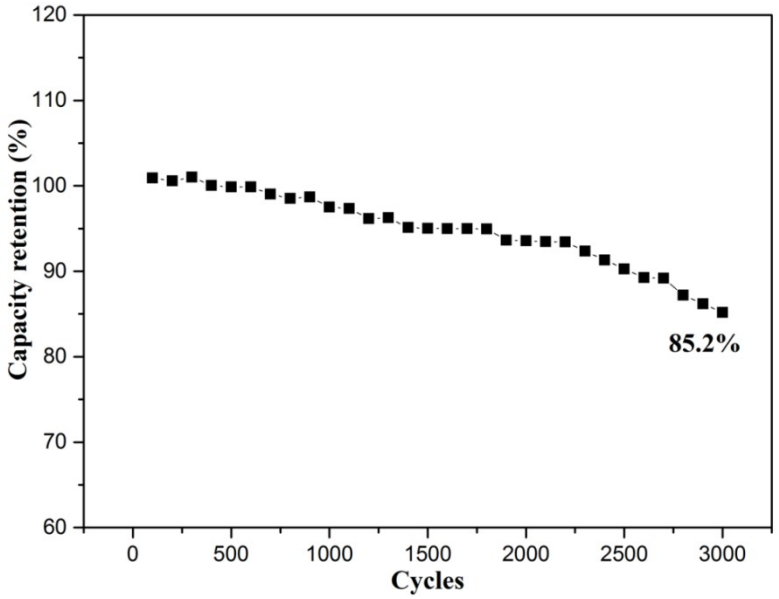

Figure S8 Cycling performance of Ni-MOF//CNTs-COOH ABSHD at a discharge current density of 10 A g^{-1} in 3 M KOH.

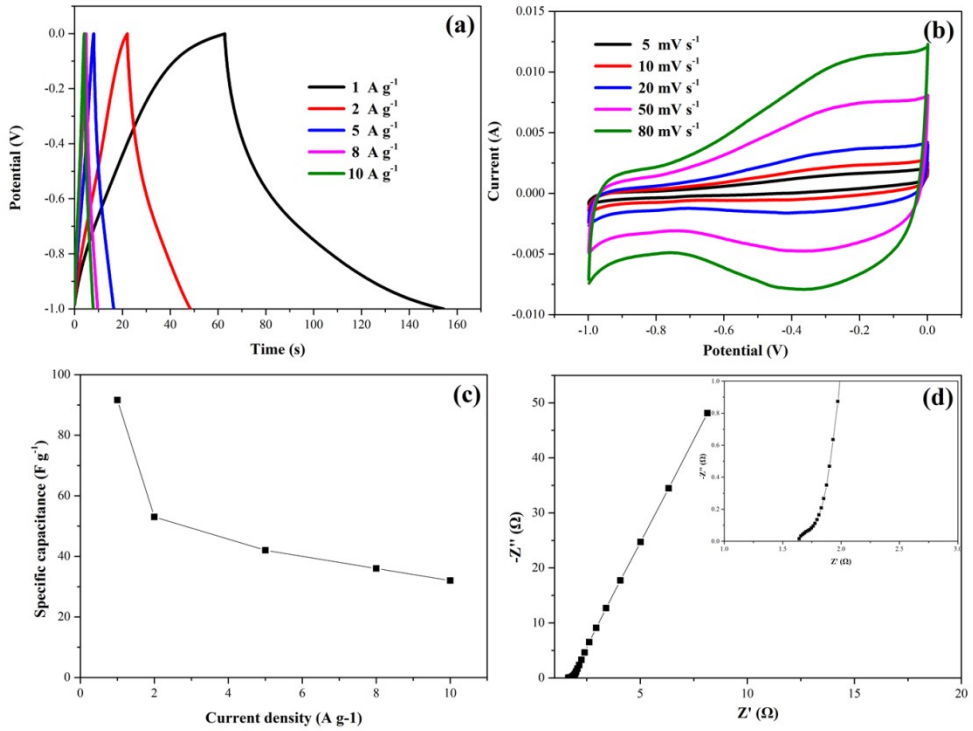

Figure S9 (a) Charge and discharge curves of AC at different current densities ranged from 1 to 10 A g^{-1}. (b) CV curves of AC at the scan rate between 5 and 80 mV s^{-1}. (c) Specific capacity as a function of current density. (d) Nyquist plots of the AC.

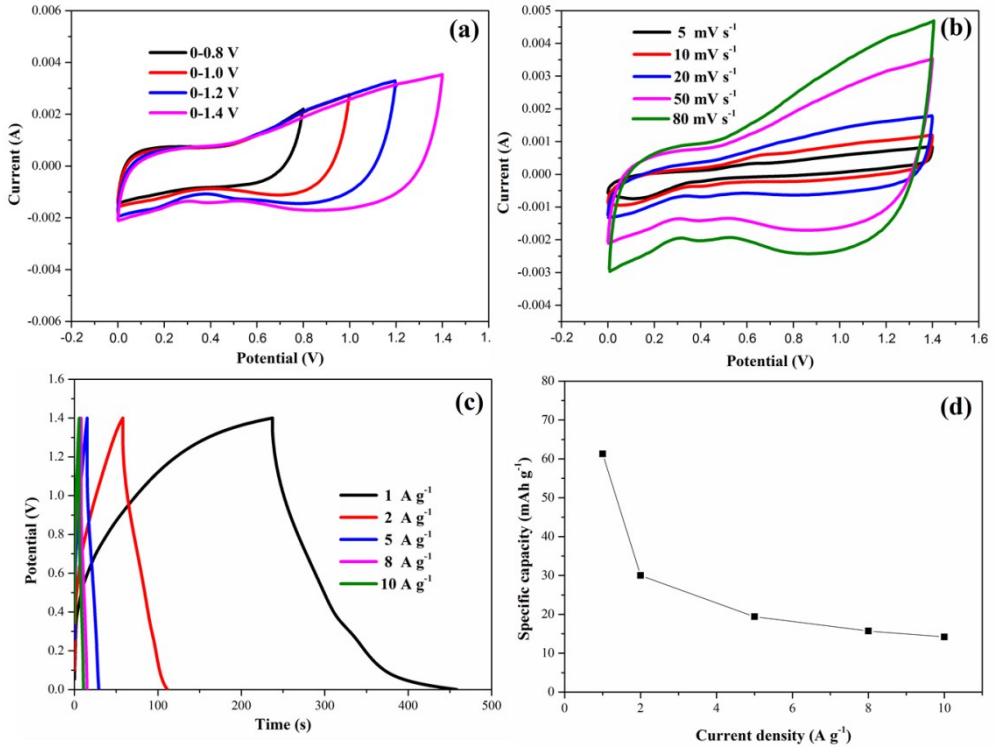

Figure S10 (a) CV curves of the optimized Ni-MOF//AC ABSHD in 3 M KOH was collected at different potential windows at a scan rate of 10 mV s^{-1}. (b) CV curves of the optimized Ni-MOF//AC ABSHD in 3 M KOH collected at various scan rates. (c) Charge–discharge curves of optimized Ni-MOF//AC ABSHD in 3 M KOH collected at various current densities. (d) Plot of the current density against the specific capacity of Ni-MOF//AC ABSHD in 3 M KOH.

[S1] X.H. Xia, C. Zhu , J. Luo, Z. Zeng, C. Guan ,C. FanNg, H. Zhang and H.J. Fan, Small 10 (2014) 766-773.

[S2] F. Zhang, L. Hao, L. Zhang, X. Zhang, Int. J. Electrochem. Sci. 6 (2011) 2943-2954.

[S3] R. Thangappan, S. Kalaiselvam, A. Elayaperumal,R. Jayavel, M. Arivanandhan, R. Karthikeyan and Y. Hayakawa, Dalton Trans. 45 (2016) 2637-2646.

[S4] M. Kolathodi, M. Palei and T.S. Natarajan, J. Mater. Chem. A 3 (2015) 7513-7522.

[S5] K. Yuan, Y. Z. Xu,J. Uihlein, G. Brunklaus, L. Shi, R. Heiderhoff, M.M. Que, M. Forster, T. Chassé, T. Pichler, T. Riedl, Y.W. Chen, U. Sche, Adv. Mater. 27 (2015) 6714-6721

[S6] Y.T. Wang, A.H. Lu, H.L. Zhang, W.C. Li, J. Phys. Chem. C 115 (2011) 5413-5421.

[S7] H.B. Li, M.H. Yu, F.X. Wang, P. Liu, Y. Liang, J. Xiao, C.X. Wang, Y. X. Tong, G.W. Yang, Nat. Commun. 4 (2013) 1894-1901.

[S8] J. Ji, L.L. Zhang, H. Ji, Y. Li, X. Zhao, X. Bai, X. Fan, F. Zhang, R.S. Ruoff, ACS Nano 7 (2013) 6237-6243.

[S9] R.R. Salunkhe, B.P. Bastakoti, C.T. Hsu, N. Suzuki, J.H. Kim, S.X. Dou, C.C.

Hu, Y. Yamauchi, Chem. Eur. J. 20 (2014) 3084-3090.
[S10] Q. Qu, P. Zhang, B. Wang, Y. Chen, S. Tian, Y. Wu, Y. Holze, J. Phys. Chem. C 113 (2009) 14020-14027.